Journal of Applied Mechanics Vol.9, pp.455-462 (August 2006) JSCE

Extended Subloading Surface Model Incorporating Elastic Boundary Concept

Seiichiro TSUTSUMI*, Masahiro TOYOSADA** and Koichi HASHIGUCHI***

* Dr. of Agr., Research Associate, Dept. of Marine System Eng., Kyushu University
(Hakozaki 6-10-1, Higashi-ku, Fukuoka 812-8581)
** Dr. of Eng., Professor, Dept. of Marine System Eng., Kyushu University
*** Dr. of Eng. and Dr. of Agr., Professor, Dept. of Agr. Eng., Kyushu University

In order to describe cyclic plasticity phenomena plastic stretching within a yield surface has to be considered, whilst conventional elastoplastic constitutive equations are only capable of describing deformation behaviour for a stress path near the monotonic/proportional loading. The subloading surface model categorized in the unconventional plasticity model and describing a smooth elastic-plastic transition would be applicable to non-proportional loading process including cyclic loading behavior of materials with a smooth yield surface. In this study the model is extended for materials exhibiting an elastic response under a particular state of stress, named elastic boundary, whilst they also exhibit a smooth elastic-plastic transition.

Key Words: *Plasticity, Cyclic mobility, Fatigue, Proportional limit, Elastic limit*

1. Introduction

The lifetime prediction of structures is one of a dominant factor to achieve an optimum design. Also, it is well known that cyclic loads produce failure of structural parts for values of stress lower than those obtained in monotonic tests. This phenomenon is so-called fatigue and is the main cause of failure of machine parts in service. Classical approaches to study these phenomena involve the characterization of total fatigue life to failure by using the stress amplitude-life (S-N) curves, while some studies are based on the fracture mechanics[1]. On the other hand, continuum description of cyclic deformation and fatigue phenomena is also useful for its understandings.

In order to simulate these fatigue phenomena the plastic stretching within a yield surface has to be described, whilst the plastic strain is induced remarkably as the stress approaches the yield stress. The traditional plastic constitutive equation, however, is capable of describing deformation behaviour for the stress path only near the monotonic/proportional loading, since its inside of the yield surface is assumed to be an elastic state. Therefore, various constitutive models, which are categorized in the framework of unconventional plasticity[2] premising that an interior of the yield surface is not the elastic domain, have been proposed up to the present. Among them[3)-9)] the subloading surface model[5)-7)] describing a smooth elastic-plastic transition has a mathematical structure applicable to the description of deformation behaviour in an arbitrary loading (including unloading and reloading) process of materials with an arbitrary smooth yield surface. The model fulfills the basic mechanical requirements[10), 11)], i.e. the continuity condition, the smoothness condition, the work rate-stiffness relaxation and the Masing effect. Furthermore, in order to describe the vertex (tangent) effect, causing the dependence of not only the magnitude but also the direction of the inelastic stretching on the stress rate, the extended vertex type of constitutive model have been proposed[12), 13)]. It has been verified that a smooth elastic-plastic transition can be well described for many kinds of soils[13)-17)]. The validity of these models were also verified for monotonic and low cycle deformation behavior of metals[18)-20)]. On the other hand, it is well known for many metallic materials that a purely elastic response, such as Hooke's type, would be observed under a particular lower state of stress, so-called proportional or elastic limit, whilst they also exhibit a smooth elastic-plastic transition as the increase of stress to the dominant yielding state. To

describe fatigue phenomena, appropriate description of deformation behavior for cyclic stresses lower than a yield stress is required.

In this article, to propose the unconventional plasticity model describing the cyclic loading behavior for the stress cycles lower than the yield stress, the subloading surface model is extended by incorporating the concept of the *elastic boundary* together with the consistent material function. The proposed model exhibits a purely elastic response under the particular state of stress and a smooth elastic-plastic transition keeping the mechanical features of the subloading surface model. The mechanical responses of the model are examined to the cyclic loading condition.

2. Extended Elasto-plastic Constitutive Model

Denoting the current configuration of the material point by $\mathbf{x}$ and the current velocity by $\mathbf{v}$, the velocity gradient is described as $\mathbf{L}=\partial \mathbf{v}/\partial \mathbf{x}$. Now the stretching and the continuum spin are defined as $\mathbf{D}$ $(=(\mathbf{L}+\mathbf{L}^{\mathrm{T}})/2)$ and $\mathbf{W}$ $(=(\mathbf{L}-\mathbf{L}^{\mathrm{T}})/2)$, respectively, where $(\ )^{\mathrm{T}}$ stands for the transpose.

2.1 Stretching and Stress Rate

In the rate-form elastoplasticity, the stretching $\mathbf{D}$ is additively decomposed into elastic stretching $\mathbf{D}^e$ and plastic stretching $\mathbf{D}^p$, i.e.

$$\mathbf{D}=\mathbf{D}^e+\mathbf{D}^p \tag{1}$$

where $\mathbf{D}^e$ is given by

$$\mathbf{D}^e=\mathbf{E}^{-1}\overset{\circ}{\boldsymbol{\sigma}} \tag{2}$$

where $\boldsymbol{\sigma}$ is the Cauchy stress. $(^{\circ})$ denotes the co-rotational rate. Here, avoiding the influence of rigid-body rotation on the constitutive relation, the following Jaumann rate is adopted.

$$\overset{\circ}{\mathbf{T}}\equiv\dot{\mathbf{T}}-\mathbf{WT}+\mathbf{TW} \tag{3}$$

Here, $\mathbf{T}$ denotes the arbitrary second-order tensor with the dimension of the stress, and $(^{\bullet})$ denotes the material-time derivative. Hereafter, the rate form of Hooke's law is adopted, and thus the elastic modulus tensor $\mathbf{E}$ in Eq. (2) is given as follows:

$$E_{ijkl}=\frac{\nu E}{(1+\nu)(1-2\nu)}\delta_{ij}\delta_{kl}+\frac{E}{2(1+\nu)}(\delta_{ik}\delta_{jl}+\delta_{il}\delta_{jk}) \tag{4}$$

where E and ν are Young's modulus and Poisson's ratio, respectively, and δ_{ij} is Kronecker's delta, i.e. $\delta_{ij}=1$ for $i=j$ and $\delta_{ij}=0$ for $i\neq j$.

2.2 Plastic Stretching

We assume that the yield condition can be written in the form:

$$f(\hat{\boldsymbol{\sigma}},\mathbf{H})=F(H) \tag{5}$$

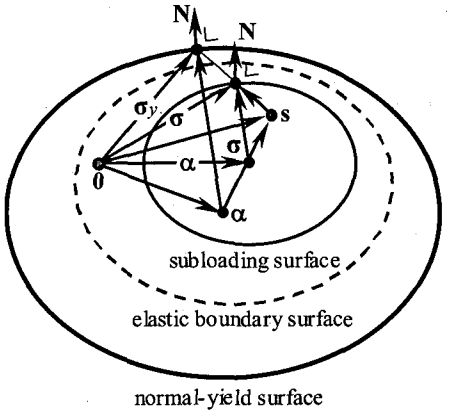

Fig. 1 The normal-yield, the subloading and the elastic limit surfaces.

where

$$\hat{\boldsymbol{\sigma}}\equiv\boldsymbol{\sigma}_y-\boldsymbol{\alpha} \tag{6}$$

The second-order tensor $\boldsymbol{\sigma}_y$ is the current stress in the plastic yielding state and $\boldsymbol{\alpha}$ is the reference point on or inside the yield surface, which is the so-called back-stress and plays the role of the kinematic hardening variable as it translates with the plastic deformation. F is the isotropic hardening/softening function, and the second-order tensor $\mathbf{H}$ and the scalar H are anisotropic and isotropic hardening variables, respectively. The kinematic hardening of the yield surface describes the Bauschinger effect characterized by early re-yielding, which is mainly due to the motion of less stable dislocations, such as piled-up dislocations. The isotropic hardening of the subloading surface represents the global work-hardening associated with the formation of stable dislocation structures, such as cell walls.

Let it be assumed that the loading function $f(\hat{\boldsymbol{\sigma}},\mathbf{H})$ is homogeneous of degree one in the tensor $\hat{\boldsymbol{\sigma}}$. Then, if $\mathbf{H}$=const., the yield surface keeps a similar shape. Drucker (1988) defined unconventional elastoplasticity as the extended elastoplasticity such that the interior of the yield surface is not a purely elastic domain, but plastic deformation is induced by the rate of stress inside the yield surface[2]. In the subloading surface model[7], the conventional yield surface is renamed to the normal-yield surface, since its interior is not regarded as a purely elastic domain.

Now, let the subloading surface be introduced, which always passes through the current stress point $\boldsymbol{\sigma}$. The subloading surface keeps the similar shape to the normal-yield surface and the positioning of similarity to the normal-yield surface with respect to the similarity-center $\mathbf{s}$. The normal-yield and subloading surfaces are illustrated in Fig. 1, where $\boldsymbol{\sigma}_y$ is regarded as the conjugate stress of the

current stress $\boldsymbol{\sigma}$ on the normal-yield surface at which the normalized outward-normal $\mathbf{N}$ is the same as that at the current stress on the subloading surface. The similarity of these surfaces possesses the following geometrical properties.

i) All lines connecting an arbitrary point inside the subloading surface and its conjugate point inside the normal-yield surface, join at the similarity-center $\mathbf{s}$ which is the origin of the stress space in the present case.

ii) All of the ratios of length of an arbitrary line element connecting two points inside the subloading surface and that of an arbitrary conjugate line-element connecting two conjugate points inside the normal-yield surface, are identical. The ratio is called the similarity ratio which coincides with the ratio of the sizes of these surfaces.

Let the similarity ratio of the subloading surface to the normal-yield surface, which plays the role of 3-dimensional measure of the degree of approach to the normal-yield state, be called specifically the normal-yield ratio and denoted by R. Therefore $0<R<1$ corresponds to the subyield state, $R=1$ to the normal-yield state in which the stress lies on the normal-yield surface and $R=0$ to the stress state, in which the stress coincides with the similarity-center $\mathbf{s}$. Then, it holds that

$$\boldsymbol{\sigma}_y = \frac{1}{R}\{\boldsymbol{\sigma} - (1-R)\mathbf{s}\} \quad (\boldsymbol{\sigma} - \mathbf{s} = R(\boldsymbol{\sigma}_y - \mathbf{s})) \tag{7}$$

The substitution of Eq. (7) into Eq.(5) gives the expression of the subloading surface as

$$f(\bar{\boldsymbol{\sigma}}, \mathbf{H}) = RF(H) \tag{8}$$

where

$$\bar{\boldsymbol{\sigma}} \equiv \boldsymbol{\sigma} - \bar{\boldsymbol{\alpha}} \quad (= R\hat{\boldsymbol{\sigma}}) \tag{9}$$

$$\bar{\boldsymbol{\alpha}} \equiv \mathbf{s} - R(\mathbf{s} - \boldsymbol{\alpha}) \quad (\bar{\boldsymbol{\alpha}} - \mathbf{s} = R(\boldsymbol{\alpha} - \mathbf{s})) \tag{10}$$

$\bar{\boldsymbol{\alpha}}$ on or inside the subloading surface is the conjugate point of $\boldsymbol{\alpha}$ on or inside the normal-yield surface, which would correspond to the back stress of the subloading surface.

The time differentiation of Eq. (8) is given by

$$\mathrm{tr}\Big\{\frac{\partial f(\bar{\boldsymbol{\sigma}}, \mathbf{H})}{\partial \boldsymbol{\sigma}} \overset{\circ}{\bar{\boldsymbol{\sigma}}}\Big\} + \mathrm{tr}\Big\{\frac{\partial f(\bar{\boldsymbol{\sigma}}, \mathbf{H})}{\partial \mathbf{H}} \overset{\circ}{\mathbf{H}}\Big\} = \dot{R}F + RF'\dot{H} \tag{11}$$

where $\mathrm{tr}(\,)$ stands for the trace operation and

$$F' \equiv \frac{dF}{dH} \tag{12}$$

As observed in experiments, the stress asymptotically approaches the normal-yield surface in the plastic loading process $\mathbf{D}^p \neq \mathbf{0}$. Thus, the following evolution equation of the normal-yield ratio R in plastic loading state is assumed.

$$\dot{R} = U \,\|\mathbf{D}^p\| \quad \text{for } \mathbf{D}^p \neq \mathbf{0} \tag{13}$$

where $\|\ \|$ stands for the magnitude. It has been assumed that the function U is a monotonically decreasing function of the normal-yield ratio R, satisfying

$$U = \begin{cases} +\infty & \text{for } R = 0, \\ 0 & \text{for } R = 1, \\ (U < 0 & \text{for } R > 1). \end{cases} \tag{14}$$

The function U satisfying Eq. (14) has been simply assumed to be given by

$$U = -m \ln R \tag{15}$$

where m is a material constant prescribing the approaching rate of the current stress to the normal-yield surface with plastic deformation. It has been verified for the models adopting Eq. (15) that the mechanical responses of soils can be well described for monotonic and cyclic loadings far lager than yield stress[13)-16)].

Let the associated flow rule be adopted for the plastic stretching $\mathbf{D}^p$ as

$$\mathbf{D}^p = \lambda \mathbf{N} \tag{16}$$

where λ is the positive proportionality factor and $\mathbf{N}$ is the normalized outward normal of the subloading surface, i.e.

$$\mathbf{N} \equiv \frac{\partial f(\bar{\boldsymbol{\sigma}}, \mathbf{H})}{\partial \boldsymbol{\sigma}} \Big/ \left\| \frac{\partial f(\bar{\boldsymbol{\sigma}}, \mathbf{H})}{\partial \boldsymbol{\sigma}} \right\| \quad (\|\mathbf{N}\| = 1) \tag{17}$$

Substituting Eqs. (13) and (16) into Eq. (11), the positive plastic multiplier λ is given by

$$\lambda \equiv \frac{\mathrm{tr}(\mathbf{N}\overset{\circ}{\boldsymbol{\sigma}})}{M^p} \tag{18}$$

where the plastic modulus M^p is given as follows:

$$M^p \equiv \mathrm{tr}\Big[\mathbf{N}\Big(\Big\{\frac{F'}{F}h - \frac{1}{RF}\mathrm{tr}\Big(\frac{\partial f(\bar{\boldsymbol{\sigma}}, \mathbf{H})}{\partial \mathbf{H}}\mathbf{h}\Big) + \frac{U}{R}\Big\}\bar{\boldsymbol{\sigma}} + \bar{\mathbf{a}}\Big)\Big] \tag{19}$$

where h, $\mathbf{h}$ are $\bar{\mathbf{a}}$ functions of the stress, plastic internal-state variables and $\mathbf{N}$ of degree one. These are related by

$$h \equiv \frac{\dot{H}}{\lambda}, \quad \mathbf{h} \equiv \frac{\overset{\circ}{\mathbf{H}}}{\lambda} \tag{20}$$

$$\bar{\mathbf{a}} \equiv \frac{\overset{\circ}{\bar{\boldsymbol{\alpha}}}}{\lambda} = R\mathbf{a} + (1-R)\mathbf{z} - U(\mathbf{s} - \boldsymbol{\alpha}) \tag{21}$$

$$\mathbf{a} \equiv \frac{\overset{\circ}{\boldsymbol{\alpha}}}{\lambda}, \quad \mathbf{z} \equiv \frac{\overset{\circ}{\mathbf{s}}}{\lambda} \tag{22}$$

The stretching $\mathbf{D}$ is given from Eqs. (1), (2), (16) and (18) as

$$\mathbf{D} = \mathbf{E}^{-1}\overset{\circ}{\boldsymbol{\sigma}} + \frac{\mathrm{tr}(\mathbf{N}\overset{\circ}{\boldsymbol{\sigma}})}{M^p}\mathbf{N} \tag{23}$$

The positive proportionality factor in the associated flow rule of Eq. (16) is expressed in terms of the stretching $\mathbf{D}$, rewriting λ by Λ, as follows:

$$\Lambda = \frac{\mathrm{tr}(\mathbf{NED})}{M^p + \mathrm{tr}(\mathbf{NEN})} \tag{24}$$

The inverse expression, i.e. the analytical expression of the stress-rate in terms of the stretching is obtained as follows:

$$\mathring{\boldsymbol{\sigma}} = \mathbf{ED} - \frac{\mathrm{tr}(\mathbf{NED})}{M^p + \mathrm{tr}(\mathbf{NEN})}\mathbf{EN} \tag{25}$$

The loading criterion is given as follows:

$$\left.\begin{aligned} &\mathbf{D}^p \neq \mathbf{0}:\ \Lambda > 0, \\ &\mathbf{D}^p = \mathbf{0}:\ \Lambda \leq 0, \end{aligned}\right\} \tag{26}$$

which is applicable not only to a hardening state but also to a perfectly-plastic and a softening state. The mechanical background of the loading criterion of Eq. (26) has been examined[21].

Subloading surface model was applied to the prediction of deformation behavior and shear band formation analysis of soils[13),15)-17)]. The validity of this model was also verified for monotonic and low cycle stress behavior of metals[18)-19)].

2.3 Translation Rule of Similarity Center

The similarity-center $\mathbf{s}$ is required to translate with plastic deformation in order to describe realistically the cyclic loading behavior exhibiting the so-called Masing effect. This translation rule for $\mathbf{s}$ is described below.

The following inequality must hold since the similarity-center $\mathbf{s}$ has to lie inside the normal-yield surface[7].

$$f(\hat{\mathbf{s}}, \mathbf{H}) \leq F(H) \tag{27}$$

where

$$\hat{\mathbf{s}} \equiv \mathbf{s} - \boldsymbol{\alpha} \tag{28}$$

Let the ultimate state $f(\hat{\mathbf{s}}, \mathbf{H}) = F(H)$ be considered, in which the similarity-center $\mathbf{s}$ just lies on the normal-yield surface, and thus there exists the possibility that the similarity-center $\mathbf{s}$ goes out from the normal-yield surface. The time differentiation of Eq. (27) in the ultimate state gives:

$$\mathrm{tr}\left[\frac{\partial f(\hat{\mathbf{s}}, \mathbf{H})}{\partial \mathbf{s}}\left(\mathring{\hat{\mathbf{s}}} - \mathring{\boldsymbol{\alpha}} + \frac{1}{F}\left\{\mathrm{tr}\left(\frac{\partial f(\hat{\mathbf{s}}, \mathbf{H})}{\partial \mathbf{H}}\mathring{\mathbf{H}}\right) - F'\dot{H}\right\}\hat{\mathbf{s}}\right]\right] \leq 0$$
$$\text{for } f(\hat{\mathbf{s}}, \mathbf{H}) = F(H) \tag{29}$$

The inequality (27) or (29) is called the enclosing condition for the similarity-center. In the ultimate state $f(\hat{\mathbf{s}}, \mathbf{H}) = F(H)$; the vector $\boldsymbol{\sigma}_y - \mathbf{s}$ $(= (\boldsymbol{\sigma} - \mathbf{s})/R)$ makes an obtuse angle with the vector $\partial f(\hat{\mathbf{s}}, \mathbf{H})/\partial \mathbf{s}$, which is the outward-normal to the similarity-center surface. Noting this fact and considering the fact that the similarity-center moves only with the plastic deformation, the following equation fulfilling the inequality (29) is assumed:

$$\mathring{\hat{\mathbf{s}}} - \mathring{\boldsymbol{\alpha}} + \frac{1}{F}\left\{\mathrm{tr}\left(\frac{\partial f(\hat{\mathbf{s}}, \mathbf{H})}{\partial \mathbf{H}}\mathring{\mathbf{H}}\right) - F'\dot{H}\right\}\hat{\mathbf{s}} = C \,/\!/\, \mathbf{D}^p \,/\!/\, (\boldsymbol{\sigma} - \mathbf{s}) \tag{30}$$

where C is a material function of the stress and the plastic internal variables in general. The translation rule of the similarity-center is now derived as follows:

$$\mathring{\hat{\mathbf{s}}} = C \,/\!/\, \mathbf{D}^p \,/\!/\, (\boldsymbol{\sigma} - \mathbf{s}) + \mathring{\boldsymbol{\alpha}} - \frac{1}{F}\left\{\mathrm{tr}\left(\frac{\partial f(\hat{\mathbf{s}}, \mathbf{H})}{\partial \mathbf{H}}\mathring{\mathbf{H}}\right) - F'\dot{H}\right\}\hat{\mathbf{s}} \tag{31}$$

In this study the function C is assumed to be given by

$$C = -c \ln R \tag{32}$$

where c (>0) is a material constant prescribing the approaching rate of the similarity-center $\mathbf{s}$ to the current stress.

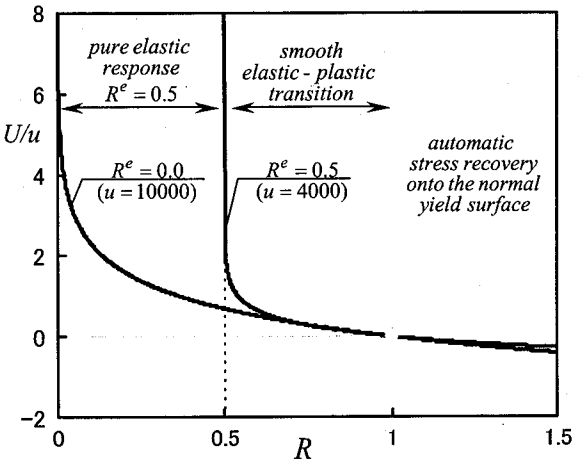

Fig. 2 The function U in the evolution rule of the similarity-ratio R.

2.4 Introduction of Elastic Boundary Concept

It is well known for many metallic materials that a elastic response, such as Hooke's type, would be observed under a particular lower state of stress, so-called proportional or elastic limit, and they also exhibit a smooth elastic-plastic transition as the increase of stress to the dominant yielding state. Following these facts the subloading surface model, categorized in the unconventional plasticity model and describing a smooth elastic-plastic transition, is extended to describe an elastic response. Here it should be noted that the terminologies of proportional or elastic limit are often used in an obscure style, both of which are not representing an elastic mechanical response of materials, since the former one guarantees only a proportionality of stress-strain relation and the later is often defined as the minimum stress inducing a particular amount of measured small inelastic strain.

Now, the concept of the *elastic boundary* is proposed, in which the elastic response is assumed under the following condition:

$$f(\overline{\boldsymbol{\sigma}}, \mathbf{H}) \leq R^e F(H) \quad (R \leq R^e) \tag{33}$$

R^e is a material function of the stress and the plastic internal variables in general, which controls the size of the elastic boundary surface. Furthermore, the function U in Eq. (13) is required to satisfy the following relations:

$$U=\begin{cases}+\infty \text{ for } R=R^e,\\ 0 \text{ for } R=1,\\ (U<0 \text{ for } R>1).\end{cases} \tag{34}$$

U is assumed to be a monotonically decreasing function of R. It should be noted that $R \le R^e$ corresponds to the elastic state, and then R is simply calculated by Eq. (8). On other hand, R=1 corresponds to the normal-yield state in which the stress exists on the normal-yield surface. The function U satisfying the relation of Eq. (34) is simply given in this study as

$$U=-u\ln\left(\frac{R-R^e}{1-R^e}\right) \text{ for } R \ge R^e \tag{35}$$

where u (>0) is a material constant prescribing the approaching rate of the current stress to the normal-yield surface (see. Fig. 2). In the case of R^e=0, Eqs. (34) and (35) coincides with Eqs. (14) and (15), respectively, and then these model results in the conventional subloading surface model without a pure elastic response except for R=0 and neutral/unloading situations. On the other hand, the model adopting R^e=1 falls within the framework of conventional plasticity without a smooth elastic-plastic transition. In case of the R>1, a stress is automatically drawn back to the normal-yield surface since it is formulated that $\dot{R} > 0$ for $R < 1$ (subyield state) and $\dot{R} < 0$ for $R > 1$ (over the normal-yield state). Thus, a rough numerical calculation with a large loading step is allowed in the subloading surface model.

The plastic stretching $\mathbf{D}^p$ in Eq. (16) with Eqs. (13) and (35) are formulated so as to be gradually induced as the similarity-ratio R approaches from the elastic boundary R^e to unity, i.e. as the stress approaches closely the normal-yield surface, so exhibiting the smooth elastic-inelastic transition. Thus, the extended subloading surface model proposed in this study fulfills the smoothness condition[10), 11)] meaning that the stress rate-stretching relation (or the stiffness tensor) changes continuously for a continuous change of stress state. Thus, it would be applicable to a general loading process for materials with an arbitrary smooth yield surface.

3. Constitutive Equation of Metals

Based on the equations formulated in Chapter 2, the constitutive equation for metals will be formulated in this section. We adopt the von Mises type of loading function $f(\overline{\boldsymbol{\sigma}})$ and the isotropic-kinematic hardening with $\mathbf{H}=\mathbf{0}$ for the subloading surface:

$$f(\overline{\boldsymbol{\sigma}})=RF(H) \tag{36}$$

where

$$f(\overline{\boldsymbol{\sigma}})=\sqrt{\frac{2}{3}}\,\|\overline{\boldsymbol{\sigma}}^*\| \tag{37}$$

$$\mathring{\boldsymbol{\alpha}}=a_1\left(a_2\frac{\boldsymbol{\sigma}^*}{\|\overline{\boldsymbol{\sigma}}^*\|}-\boldsymbol{\alpha}\right)\|\mathbf{D}^p\| \tag{38}$$

$$F=F_0[1+h_1\{1-\exp(-h_2H)\}] \tag{39}$$

$$\dot{H}=\sqrt{\frac{2}{3}}\,\|\mathbf{D}^p\| \tag{40}$$

$\overline{\boldsymbol{\sigma}}^*$ stands for

$$\overline{\boldsymbol{\sigma}}^*\equiv\overline{\boldsymbol{\sigma}}-\frac{1}{3}\mathrm{tr}(\overline{\boldsymbol{\sigma}})\mathbf{I} \tag{41}$$

h_1, h_2, a_1 and a_2, are material constants, and F_0 is initial value of F.

The functions in the constitutive Eq. (25) are given from Eqs. (37)-(40) as

$$\mathbf{N}=\frac{\boldsymbol{\sigma}^*}{\|\overline{\boldsymbol{\sigma}}^*\|} \tag{42}$$

$$M^p=\mathrm{tr}\left[\mathbf{N}\left\{\left(\sqrt{\frac{2}{3}}\frac{F'}{F}h+\frac{U}{R}\right)\overline{\boldsymbol{\sigma}}+\overline{\mathbf{a}}\right\}\right] \tag{43}$$

$$F'=F_0h_1h_2\exp(-h_2H) \tag{44}$$

$$\mathbf{a}=a_1\left(a_2\frac{\boldsymbol{\sigma}^*}{\|\overline{\boldsymbol{\sigma}}^*\|}-\boldsymbol{\alpha}\right) \tag{45}$$

Numerical simulations of stress-strain responses were conducted using the present model.

4. Mechanical Responses

Numerical simulations of stress-strain responses were conducted under uniaxial condition. The calculated results were compared to the corresponding experimental data for aluminum alloys.

4.1 Material

The material used in this study was Al-Mg alloy A5083, a commercial aluminum alloy. Among aluminum alloys, A5083 has been used widely for liquefied situations

Table 1 Tensile properties of A5083 (MPa, %)

Material	E	σ_Y	σ_B	σ_F	ε
A 5083	72000	183	335	396	15.5

E : Young's modulus; σ_Y : yield stress; σ_B : tensile strength; ε : elongation. (The number of tested specimens was 3.)

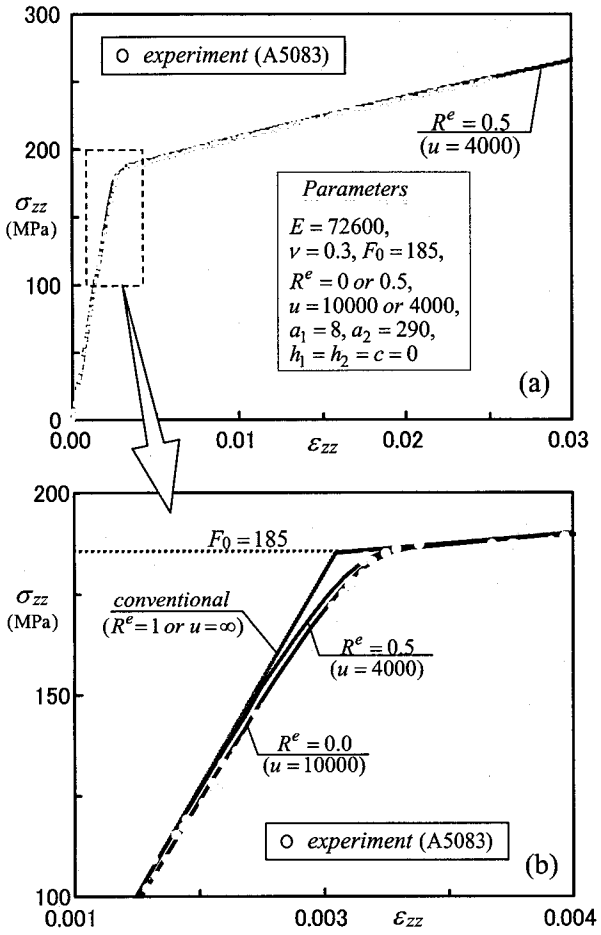

Fig. 3 Stress strain relations of the experimental result (A5083) and the numerical models under uniaxial extension condition.

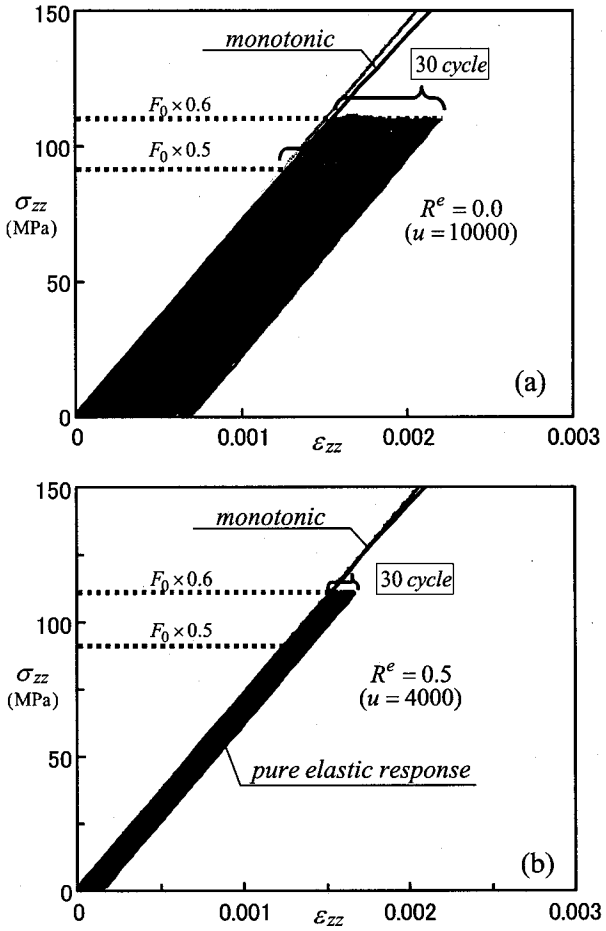

Fig. 4 Cyclic loading responses of (a) conventional subloading surface model; (b) proposed model.

because of its excellent strength and weldability. In addition to austenite stainless steels, aluminum alloys, which have good resistance to embrittlement by hydrogen, are considered. The tensile properties of A5083 at room temperature are obtained for round bar as in Table 1.

4.2 Material and Model Responses

Fig. 3(a) shows the stress-strain relation of a monotonic tension test of A5083, together with the calculated result by the proposed model. Fig. 3 (b) shows the expanded stress-strain relation around the yield stress of Fig. 3(a) by the conventional subloading surface (R^e=0) and the extend ($R^e \neq 0$) models, selecting material parameters as follows:

$$E = 72600, \quad \nu = 0.3, \quad F_0 = 185,$$
$$a_1 = 8, a_2 = 290, \quad (h_1 = h_2 = c = 0)$$
$$\left.\begin{matrix} R^e = 0 \\ u = 10000 \end{matrix}\right\} \text{ or } \left.\begin{matrix} R^e = 0.5 \\ u = 4000 \end{matrix}\right\}$$

The calculated result by the classical plasticity model (R^e=1 or $u=\infty$) exhibits a bi-linear like response, while the experimental results do not. On the other hand the unconventional plasticity models (R^e=0 or R^e=0.5) gives better results, and the smooth elastic-plastic transition of stress-strain relation is predicted quite well by the subloading surface mode with and without elastic boundary parameter. Then it can be concluded that the stress-strain relation of A5083 exhibiting smooth elasto-plastic transition under monotonic loading condition can be reproduced well by the unconventional plasticity models.

In order to examine the difference between the conventional and the extended model in the performance of describing mechanical responses for cyclic stress conditions lower than yield stress, in which conventional plasticity models (R^e=1) cannot describe any plastic deformation, the numerical simulations were conducted by conventional (R^e=0) and extended ($R^e \neq 0$) subloading surface model. Figure 4 shows the stress-strain relation under one-side cyclic loading condition for two maximum levels of deviatoric stresses $F_0 \times 0.5$ and $F_0 \times 0.6$

corresponding to the cyclic stress states $0 \le R \le 0.5$ and $0 \le R \le 0.6$, respectively. Thirty times of each cyclic loading between 0 to maximum levels are applied. It can be seen from Fig. 4 (b) that the elastic responses are obtained for the cyclic stress lower than the stress state R^e. Compared with the response of the conventional subloading surface model (R^e=0) in Fig 5(a), the larger decreases of axial strain under the cyclic loading are predicted by introducing the material constant R^e on the magnitude of the elastic boundary surface.

5. Concluding Remarks

A constitutive model within unconventional plasticity has been presented. The model is based on the subloading surface model and extended by incorporating elastic boundary concept. The validity of the present model has been confirmed by comparing the results of numerical simulations of stress-strain responses under uniaxial extension condition and the corresponding experimental observations on aluminum alloy. The mechanical responses under cyclic loading conditions are also discussed. The highlights of this model are summarized as follows.

1. The proposed model incorporating elastic boundary concept describes a smooth elastic-plastic transition observed in the uniaxial extension test of aluminum alloys.
2. The elastic responses are described for the lower stress state than that of R^e, whilst conventional subloading surface model cannot.

REFERENCES

1) Toyosada, M., Gotoh, K. and Niwa, T., Fatigue crack propagation for a through thickness crack: a crack propagation law considering cyclic plasticity near the crack tip, *Int. J. Fatigue*, Vol. 26, pp. 983-992, 2004.

2) Drucker, D.C., Conventional and unconventional plastic response and representation, *Appl. Mech. Rev.* (ASME), Vol. 41, pp. 151-167, 1988.

3) Dafalias, Y.F. and Herrmann, L.R., A bounding surface soil plasticity model, *Proc. Int. Symp. Soils under Cyclic Trans. Load.*, Swansea, pp. 335-345, 1980.

4) Dafalias, Y.F. and Popov, E.P., A model of nonlinearly hardening materials for complex loading, *Acta Mech.*, Vol. 21, pp. 173-192, 1975.

5) Hashiguchi, K., Constitutive equations of elastoplastic materials with elastic-plastic transition, *J. Appl. Mech.* (ASME) 47, pp. 266-272, 1980.

6) Hashiguchi, K., Constitutive equations of elastoplastic materials with anisotropic hardening and elastic-plastic transition, *J. Appl. Mech.* (ASME) 48, pp. 297-301, 1981.

7) Hashiguchi, K., Subloading surface model in unconventional plasticity, *Int. J. Solid Struct.*, Vol. 25(8), pp. 917-945, 1989.

8) Iwan, W.D., On a class of models for the yielding behavior of continuous and composite systems, *J. Appl. Mech.* (ASME), Vol. 34, pp. 612-617, 1967.

9) Mroz, Z., On the description of anisotropic workhardening, *J. Mech. Phys. Solids*, Vol. 15, pp. 163-175, 1967.

10) Hashiguchi, K., Fundamental requirements and formulation of elastoplastic constitutive equations with tangential plasticity, *Int. J. Plasticity*, Vol. 9, pp. 525-549, 1993.

11) Hashiguchi, K., Mechanical requirements and structures of cyclic plasticity models, *Int. J. Plasticity*, Vol. 9, pp. 721-748, 1993.

12) Hashiguchi, K. and Tsutsumi, S., Elastoplastic constitutive equation with tangential stress rate effect, *Int. J. Plasticity*, Vol. 17, pp. 117-145, 2001.

13) Tsutsumi, S. and Hashiguchi, K., General non-proportional loading behavior of soils, *Int. J. Plasticity*, Vol. 21(10), pp. 1941-1969, 2005.

14) Asaoka, A., Nakano, M., Noda, T. and Kaneda, K., Delayed compression/consolidation of natural clay due to degradation of soil structure, *Soils and Foundations*, Vol. 40(3), pp. 75-85, 2000.

15) Hashiguchi, K. and Chen, Z.-P., Elastoplastic constitutive equation of soils with the subloading surface and the rotational hardening, *Int. J. Numer. Anal. Meth. Geomech.*, Vol. 22, pp. 197-227, 1998.

16) Hashiguchi, K., Saitoh, K., Okayasu, T. and Tsutsumi, S., Evaluation of typical conventional and unconventional plasticity models for the prediction of softening behavior of soils, *Geotechnique*, Vol. 52, pp. 561-573, 2002.

17) Hashiguchi, K. and Tsutsumi, S., Shear band formation analysis in soils by the subloading surface model with tangential stress rate effect, *Int. J. Plasticity*, Vol. 19(10), pp. 1651–1677, 2003.

18) Hashiguchi, K., Protasov, A. Y. and Okayasu, T., Post-localization analysis by the subloading surface model with tangential stress rate effect, *Materials Sci. Res. Int.*, Vol. 7, 265-272, 2001.

19) Hashiguchi, K. and Yoshimaru, T., A generalized formulation of the concept of nonhardening region, *Int. J. Plasticity*, Vol. 11(4), pp. 347-365, 1995.

20) Tsutsumi, S., Toyosada, M., Gotoh, K. and Hashiguchi, H., FE analysis on mechanical

fatigue, *Proc. Int. Conf. Computational & Experimental Engineering & Sciences*, pp. 1380-1385, 2005.

21) Hashiguchi, K., On the loading criterion, *Int. J. Plasticity,* Vol. 10, pp. 871-878, 1994.

(Received: April 13, 2006)